0026-895X/05/6803-644–651$20.00
MOLECULAR PHARMACOLOGY
Vol. 68, No. 3
13763/3048546
Mol Pharmacol 68:644–651, 2005
Printed in U.S.A.

CYP2C9 Genotype-Dependent Effects on in Vitro Drug-Drug Interactions: Switching of Benzbromarone Effect from Inhibition to Activation in the CYP2C9.3 Variant

Matthew A. Hummel, Charles W. Locuson, Peter M. Gannett, Dan A. Rock, Carrie M. Mosher, Allan E. Rettie, and Timothy S. Tracy

Department of Experimental and Clinical Pharmacology, University of Minnesota, Minneapolis, Minnesota (M.A.H., C.W.L., T.S.T.); Department of Basic Pharmaceutical Sciences, West Virginia University, Morgantown, West Virginia (P.M.G.); Global Pharmacokinetics, Dynamics, and Metabolism, Pfizer, Inc., St. Louis, Missouri (D.A.R.); and Department of Medicinal Chemistry, University of Washington, Seattle, Washington (C.M.M., A.E.R.)

Received April 13, 2005; accepted June 13, 2005

ABSTRACT

The CYP2C9.3 variant exhibits marked decreases in substrate turnover compared with the wild-type enzyme, but little is known regarding the effect this variant form may have on the occurrence of drug-drug interactions. To examine this possibility, the effect of the potent CYP2C9 inhibitor, benzbromarone, was studied with regard to CYP2C9.1- and CYP2C9.3-mediated flurbiprofen metabolism to evaluate whether the variant enzyme exhibits differential inhibition kinetics. Although benzbromarone inhibited CYP2C9.1 activity as expected, CYP2C9.3-mediated flurbiprofen 4′-hydroxylation was activated in the presence of benzbromarone. T_1 relaxation studies revealed little change in distances of flurbiprofen protons from the heme iron of either CYP2C9.1 or CYP2C9.3 in the presence of benzbromarone compared with flurbiprofen alone. Spectral binding studies were also performed to investigate whether benzbromarone affected substrate binding, with the addition of benzbromarone having little effect on flurbiprofen-binding affinity in both CYP2C9.1 and CYP2C9.3. Docking studies with the 2C9.1 structure crystallized with a closed active site identified multiple but overlapping subsites with sufficient space for benzbromarone binding in the enzyme when flurbiprofen was positioned closest to the heme. If the closed conformation of 2C9.3 is structurally similar to 2C9.1, as expected for the conservative I359L mutation, then the dynamics of benzbromarone binding may account for the switching of drug interaction effects. In conclusion, the I359L amino acid substitution found in CYP2C9.3 not only reduces metabolism compared with CYP2C9.1 but can also dramatically alter inhibitor effects, suggesting that differential degrees of drug inhibition interactions may occur in individuals with this variant form of CYP2C9.

Prediction of drug interactions involving the cytochrome P450 (P450) enzyme system requires an accurate estimation of the inhibition kinetics. New compounds are routinely tested in an in vitro system using liver microsomes or purified enzymes against P450 isoform-specific probe substrates to gauge which and to what extent a particular P450 isoform is inhibited. One probe substrate is often selected for each P450 isoform. However, it is known that the CYP2C9 and CYP3A4 isoforms exhibit atypical kinetic profiles, presumably because of the binding of more than one molecule within its active site (Shou et al., 1994, 1999, 2001; Hutzler et al., 2001, 2003; Galetin et al., 2002; Nakamura et al., 2002). The crystal structure of CYP2C9 has been solved and has facilitated visualization of how multiple substrates may bind within the active site (Williams et al., 2003; Wester et al., 2004). This unusual occurrence leads to atypical kinetic phenomena, such as heterotropic or homotropic cooperation (a.k.a., activation), substrate inhibition, and biphasic kinetics, making correlation to the in vivo situation more difficult (Hutzler et al., 2001; Tracy et al., 2002). The ability of CYP2C9 to accept multiple molecules into its active site, because of its active site volume, may make it possible for a potential inhibitor of one substrate to have no effect on metabolism of the target substrate but still inhibit the metabolism of a different target substrate. This can result in substrate-dependent inhibition for a given inhibitor.

This study was supported in part by National Institutes of Health grants GM069753 and GM063215 (T.S.T) and GM032165 (A.E.R.), the University of Minnesota School of Medicine National Science Foundation grant BIR-961477, and the Minnesota Medical Foundation.

Article, publication date, and citation information can be found at http://molpharm.aspetjournals.org.

doi:10.1124/mol.105.013763.

ABBREVIATIONS: P450, cytochrome P450; HPLC, high pressure liquid chromatography; PCR, polymerase chain reaction; NMR, nuclear magnetic resonance.

Allelic variants, such as CYP2C9.3, exhibit reduced substrate turnover that can lead to alterations in in vivo pharmacokinetics (Haining et al., 1996; Steward et al., 1997; Yamazaki et al., 1998; Takanashi et al., 2000; Higashi et al., 2002). Furthermore, the altered pharmacokinetics caused by this polymorphism can result in profound effects on the therapeutic outcome of clinically important drugs, such as warfarin (Higashi et al., 2002). In addition, we have previously reported that the CYP2C9 allelic variants exhibit differential degrees of dapsone-mediated activation of flurbiprofen metabolism, with CYP2C9.3 showing the greatest percentage increase in flurbiprofen 4′-hydroxylation activity compared with CYP2C9.1, CYP2C9.2, and CYP2C9.5 (Hummel et al., 2004a). However, little is known regarding whether enzyme inhibition also exhibits differential effects among the CYP2C9 variants, particularly the clinically relevant CYP2C9.3 enzyme.

To test the hypothesis that differential inhibition of CYP2C9 variants may occur, metabolism of the model CYP2C9 substrate flurbiprofen (Tracy et al., 1995, 1996) was studied in the presence of the potent CYP2C9 inhibitor benzbromarone (Locuson et al., 2003, 2004) in both CYP2C9.1 and CYP2C9.3 enzyme. To evaluate possible reasons for observed differences, potential changes in substrate-enzyme-inhibitor interactions were also studied by measuring binding affinities (K_s) and proton distances from the P450 heme and by conducting preliminary docking studies.

Materials and Methods

Acetonitrile, potassium phosphate, glycerol, and EDTA were purchased from Fisher Scientific Co. (Pittsburgh, PA). NADPH, dilauroylphosphatidylcholine, poly(vinylpyrrolidone), benzbromarone, and sodium dithionite were obtained from Sigma-Aldrich (St. Louis, MO). D_2O was obtained from Cambridge Isotopes Laboratory (Andover, MA). (*S*)-Flurbiprofen, 4′-hydroxyflurbiprofen, and 2-fluoro 4-biphenyl acetic acid were gifts from Pfizer, Inc. (New York, NY). Centricon MW cut-off filters were obtained from Millipore Corporation (Billerica, MA). Human P450 oxidoreductase and human cytochrome b_5 were purchased from Invitrogen (Carlsbad, CA).

Enzyme Expression and Incubation Conditions. The *2C9.1* gene was subcloned into the pCWori$^+$ vector from the original baculovirus transfer vector pUC19 (Haining et al., 1999) using a single PCR with the following primers: forward, 5′-CCA TCG ATC ATA TGG CTC TGT TAT TAG CAG TTT TTC TCT GTC TCT CAT GTT TGC TTC TCC TTT C-3′; and reverse, 5′-TCT GTC GAC ACA GGA ATG AAG CAC AGC TGG TAG AAG-3′. The forward primer encoded the MALLLAVFL N-terminal sequence of recombinant bovine P450 17α to enhance expression in *Escherichia coli* (Barnes et al., 1991). NdeI and SalI restriction sites were also engineered into the forward and reverse primers, respectively, to facilitate downstream subcloning. The PCR product and pCWori$^+$ vector were digested with NdeI and SalI, gel-purified, ligated together for 10 min at 25°C, and finally transformed into DH5α F′IQ cells. The *2C9.3* construct was generated using *2C9.1* as a template. A single PCR was performed using the following primers: forward, 5′-GTC CAG AGA TAC CTT GAC CTT CTC CCC ACC AGC CTG-3′; and reverse, 5′-CAG GCT GGT GGG GAG AAG GTC AAG GTA TCT CTG GAC-3′. These primers incorporate the A→C point mutation at base position 1061 that is responsible for the Ile→Leu substitution. The final PCR product was digested with DpnI for 1 h at 37°C and then transformed into DH5α F′IQ cells. All of the constructs were verified by DNA sequencing. Protein expression in *E. coli* was carried out as described previously (Cheesman et al., 2003).

Metabolic incubations were carried out according to the methods of Tracy et al. (2002). Incubation mixtures contained 5 to 20 pmol of purified P450, NADPH reductase, and cytochrome b_5 in a 1:2:1 ratio reconstituted with dilauroylphosphatidylcholine vesicles extruded through a 200-nm pore-sized membrane. To study the effects of benzbromarone on CYP2C9.1-mediated flurbiprofen 4′-hydroxylation, six concentrations of 2 to 300 μM (*S*)-flurbiprofen were incubated with six concentrations of 0 to 300 nM benzbromarone. In the case of benzbromarone effects on CYP2C9.3-mediated flurbiprofen 4′-hydroxylation, six concentrations of 2 to 300 μM (*S*)-flurbiprofen were incubated with six concentrations of 0 to 300 nM benzbromarone. All of the incubations were conducted for 20 min at 37°C in 50 mM potassium phosphate buffer, pH 7.4, in a final volume of 200 μl. After a 3-min preincubation, reactions were initiated by the addition of NADPH (final concentration of 1 mM). Reactions were quenched by the addition of 200 μl of acetonitrile containing internal standard and 180 ng/ml 2-fluoro-4-biphenyl acetic acid as internal standard. After quenching, 40 μl of half-strength H_3PO_4 was added to the reaction mixtures. Samples were then centrifuged at 10,000 rpm for 4 min and placed into autosampler vials, and 50 μl was injected onto the HPLC system.

Metabolite Quantitation. HPLC analysis of 4′-hydroxyflurbiprofen production was conducted as described previously (Tracy et al., 2002). The HPLC system consisted of a Waters Alliance 2695XE chromatographic system and a Waters model 2475 fluorescence detector (Waters, Milford, MA). The mobile phase was pumped through a Brownlee Spheri-5 C_{18} 4.6 × 100-mm column (PerkinElmer Life and Analytical Sciences, Boston, MA) at 1 ml/min. For quantification of 4′-hydroxyflurbiprofen, the detector was set at an excitation wavelength of 260 nm and an emission wavelength of 320 nm and the mobile phase consisted of 45:55 acetonitrile/20 mM potassium phosphate, pH 3.0. The retention times for 4′-hydroxyflurbiprofen and the internal standard were approximately 2.6 and 5.6 min, respectively.

Kinetic Data Analysis. Kinetic parameters for the substrates were estimated by nonlinear regression analysis using Sigma Plot 8.0 (Systat Software, Richmond, CA). To simplify comparisons, kinetic data for activation of CYP2C9.3 as well as inhibition of CYP2C9.1-mediated flurbiprofen 4′-hydroxylation in the presence of benzbromarone were fit to a two-site model (Korzekwa et al., 1998; Hutzler et al., 2001).

$$v = \frac{V_m \times [S]}{K_m \frac{\left(1 + \frac{[B]}{K_B}\right)}{\left(1 + \frac{\beta[B]}{\alpha K_B}\right)} + [S] \frac{\left(1 + \frac{[B]}{\alpha K_B}\right)}{\left(1 + \frac{\beta[B]}{\alpha K_B}\right)}} \quad (1)$$

Appropriateness of the fits was determined by examination and comparison of the residuals, residual sum of squares, coefficients of determination, and *F* values.

Enzyme Sample Preparation for NMR. Enzyme samples for use in T_1 relaxation measurements were prepared as reported previously (Hummel et al., 2004b). Concentrated enzyme samples were diluted 50-fold into 50 mM potassium phosphate, pH 7.4, in D_2O to remove the majority of the glycerol and H_2O. CYP2C9.1 was then added to the sample tube at a concentration of 0.014 μM in a final volume of 750 μl containing either 145 μM flurbiprofen alone or 145 μM flurbiprofen plus 300 nM benzbromarone. When CYP2C9.3 was studied, the enzyme was added to the sample tube at a concentration of 0.030 μM in a final volume of 750 μl containing either 300 μM flurbiprofen alone or 300 μM flurbiprofen plus 300 nM benzbromarone. Determination of distances of the benzbromarone protons either alone or in the presence of flurbiprofen was not possible because of the insufficient sensitivity and resolution to monitor the low concentrations of benzbromarone (in nanomolar) employed in the study.

T_1 Relaxation Time Measurements. Chemical shift assignments for flurbiprofen protons (Fig. 1) were made as described previously (Hummel et al., 2004b). T_1 times of substrate protons were

determined with the NMR (Varian Inova 600 MHz Spectrometer) operating at 600.5 MHz, internally locked on the deuterium signal of the solvent. The probe was maintained at 298 K for all of the experiments except when testing for fast exchange conditions (see below). The Varian T_1 inversion-recovery sequence (d_1-180-d_2-90) was used along with presaturation of the residual HOD signal. The 90° pulse-width was calibrated on each sample. Spectra were acquired for 12 τ values (d_2) ranging from 0.0125 to 25.6 s, and a period of 10 $\times$ T_1 was used between pulses (d_1). The Varian software routines were used to determine T_1 times. Once the paramagnetic effect of the heme iron on substrate protons was measured, carbon monoxide (CO) was bubbled through the sample for 15 min and sodium dithionite was then added and allowed to equilibrate for 30 min to determine the diamagnetic contribution of the protein to the T_1 relaxation times. To ensure adequate diffusion of CO and mixing of dithionite, samples were removed from the NMR tube and treated with CO and sodium dithionite and then the sample was placed back into the NMR tube for the measurements. Stability of the enzyme as well as the CO-reduced complex was tested, and both were found to be stable for the duration of the NMR acquisition time.

T_1 measurements and the resulting calculated distances are dependent on the substrate being in fast exchange with the enzyme. The validity of this assumption can be demonstrated by conducting T_1 measurements over a range of temperatures (Regal and Nelson, 2000). Thus, T_1 measurements were performed as described above at three different temperatures (283, 298, and 310 K). Data were collected both in the absence ($1/T_{1,2C9}$) and presence ($1/T_{1,2C9+CO}$) of CO/sodium dithionite.

Proton Heme Iron Distance Calculation. Estimates for distances of protons from the heme iron of CYP2C9 were calculated using the equation $r = C[T_{1p\alpha m} f(\tau_c)]^{1/6}$, where r is the distance and C is a constant that is a function of the metal and the oxidation state and whether it is low or high spin. In this case, Fe^{3+} should be in the low-spin state; thus, the appropriate value for C is 539 (Mildvan and Gupta, 1978). T_{1p} is the portion of T_{1obs} because of paramagnetic effects alone and is given by $T_{1p}{}^{-1} = T_{1obs}(Fe^{3+})^{-1} - T_{1obs}(Fe^{2+})^{-1}$, assuming that all of the diamagnetic contribution is represented by $T_{1obs}(Fe^{2+})$ (Regal and Nelson, 2000). This assumption has been used in many similar studies and seems to be generally valid (Modi et al., 1996; Poli-Scaife et al., 1997; Shafirovich et al., 2002). The parameter α_m is equal to [P450]/(K_s + [substrate]) under conditions of fast exchange (Regal and Nelson, 2000). The flurbiprofen K_s values of 7 μM CYP2C9.1 and 14 μM CYP2C9.3 determined from visible spectroscopy were used for estimation of the parameter α_m. The correlation time (τ_c) for CYP2C9 has been reported previously (2×10^{-10} s^{-1}) (Poli-Scaife et al., 1997) and was used here.

Spectral Binding. Spectral binding studies to measure enzyme-substrate affinity were performed as reported previously (Hutzler et al., 2003). In brief, 300 pmol of enzyme along with 0.2 μg/pmol dilauroylphosphatidylcholine was placed into the sample and reference cuvettes. For determination of spectral changes at increasing concentrations of flurbiprofen, 5-μl aliquots of flurbiprofen were added to the sample cuvette, whereas 5 μl of 50 mM potassium phosphate buffer, pH 7.4, was added to the reference cuvette. After mixing, the sample and reference cuvette were allowed to equilibrate for 3 min before spectral analysis. Spectra were recorded on an Aminco DW-2000 UV-visible spectrophotometer with Olis modifications (Olis, Inc., Bogart, GA). The spectrophotometer was set to record spectra between 350 and 500-nm wavelengths with a slit-width of 6.0 nm and scan rate of 100 nm/min. The temperature was held at a constant 28°C. The difference in absorbance between the peak (~390) and trough (~420) of the observed type I-binding spectrum was calculated and plotted against flurbiprofen concentration. A binding constant (K_s) was determined by fitting the resulting data to the eq. 2.

$$\Delta A = \frac{(B_{max} \times S)}{K_s + S} \quad (2)$$

Spectral binding experiments were also performed with flurbiprofen in the presence of 300 nM benzbromarone for each enzyme.

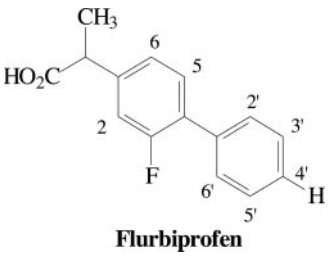

Flurbiprofen

Fig. 1. Structure of flurbiprofen with protons numbered as they are referenced within the text. The 4′-H is the site of oxidation.

Molecular Modeling. MoViT, version 8.0 (Pfizer, Inc.) was used to dock and minimize benzbromarone in the CYP2C9 crystal structure (Protein Data Bank 1R9O) (Wester et al., 2004) with flurbiprofen after importation of coordinates. The chemical structure of benzbromarone was created in ChemDraw and imported into MoViT followed by energy minimization of benzbromarone. NMR distances obtained from the T_1 NMR data were used to guide manipulations of flurbiprofen and benzbromarone. During docking, consideration was given to possible interactions between key active site residues, including Arg108, Phe114, Phe100, and Phe476. The final representation is a product of multiple energy-minimized docking iterations.

Results

The effects of benzbromarone on the 4′-hydroxylation of flurbiprofen by both CYP2C9.1 and CYP2C9.3 are presented as three-dimensional contour plots and depicted in Fig. 2, A and B. Data for both enzymes were fitted to a two-site kinetic model (eq. 1) to allow direct comparison of the kinetic parameter estimates, and the results of these estimates are presented in Table 1. The concave nature of the plot in Fig. 2A resulting from CYP2C9.1-dependent metabolism demonstrates the inhibitory effect that benzbromarone has upon the metabolism of flurbiprofen. It is surprising that an opposite effect (activation) was noted (Fig. 2B) when benzbromarone was studied as an effector of CYP2C9.3-mediated flurbiprofen hydroxylation, resulting in a convex three-dimensional contour plot. Evaluation of the kinetic parameter estimates (Table 1) presents interesting contrasts between the effects of benzbromarone in the two enzymes. The K_B for benzbromarone as an activator of flurbiprofen metabolism in CYP2C9.3 is roughly 15-fold higher than noted when benzbromarone acts as an inhibitor in the CYP2C9.1 enzyme. In the CYP2C9.1-mediated process, K_m is greatly increased (α = 5.0) by benzbromarone, whereas V_m is reduced by 50%. This type of kinetic change is typically indicative of a mixed competitive and noncompetitive type of inhibition. In the case of the activation of CYP2C9.3 by benzbromarone, K_m is greatly reduced (α = 0.14) but the V_m of flurbiprofen 4′-hydroxylation is slightly changed (β = 1.14).

To ascertain whether the changes noted in K_m for flurbiprofen hydroxylation by each of the two enzymes are accompanied by alterations in substrate affinity, spectral binding studies were conducted. The spectral binding constant (K_s) for flurbiprofen in the presence of CYP2C9.1 was 7 μM (Fig. 3A), whereas, in the presence of CYP2C9.3, the K_s for flurbiprofen was 14 μM (Fig. 4A). The addition of 300 nM benzbromarone reduced the K_s by 40% (Fig. 3B), which is roughly comparable with the magnitude of the change noted in K_m

(~20% decrease) under these same conditions. It is interesting that, despite the substantial activation of CYP2C9.3-mediated metabolism of flurbiprofen and concomitant reduction in K_m caused by the addition of benzbromarone, no changes were noted in binding affinity (K_s) of flurbiprofen with CYP2C9.3 in the presence of benzbromarone (Fig. 4, A and B). Furthermore, with the CYP2C9.3 enzyme, in the presence of flurbiprofen alone, no demonstrable peak was noted at ~390 nm, whereas, when 300 nM benzbromarone was added, a substantial ~390-nm peak was noted similar to that observed with wild-type enzyme (either in the absence or presence of benzbromarone).

T_1 NMR experiments were next conducted to determine whether benzbromarone altered the distance of the substrate (flurbiprofen) protons from the heme iron, potentially contributing to the alterations in metabolism. The estimated distances of flurbiprofen protons from the heme iron of CYP2C9.1 and CYP2C9.3 are listed in Tables 2 and 3, respectively. In the presence of CYP2C9.1, the distances of the flurbiprofen protons from the heme iron were relatively unaffected by benzbromarone. Likewise, with CYP2C9.3, the presence of 300 nM benzbromarone had little effect on distances of flurbiprofen protons to the heme iron. When studied in the presence of only 100 nM benzbromarone, similar results were noted. It is also interesting to note that the flurbiprofen protons are essentially the same distance to the

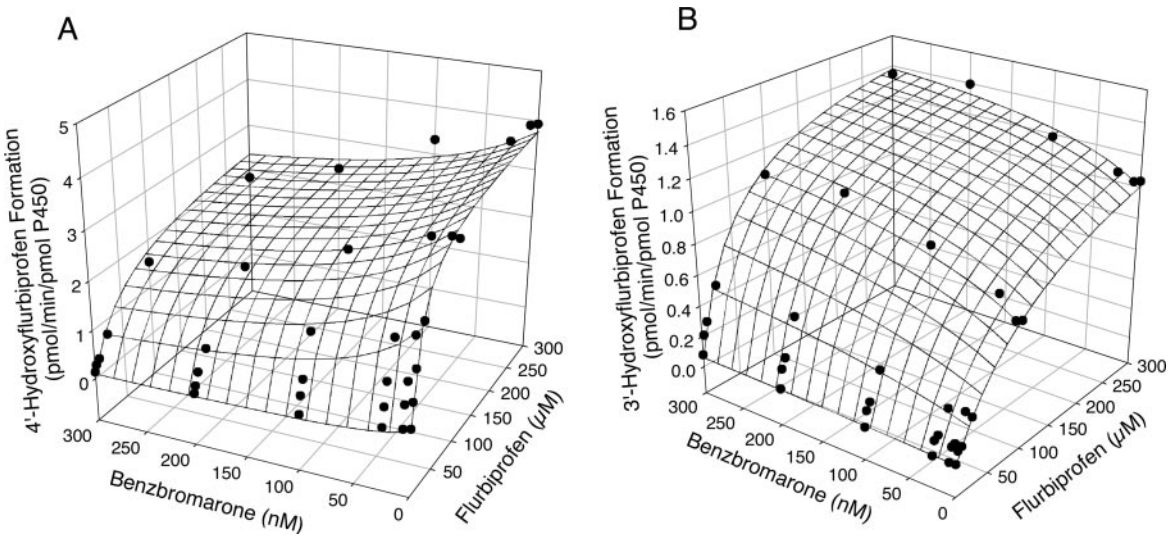

Fig. 2. Two-site model fit of the benzbromarone inhibition of CYP2C9.1 (A) and CYP2C9.3 (B). Data points represent mean of duplicate determinations.

TABLE 1

Kinetic parameter estimates for flurbiprofen 4′-hydroxylation in the presence of varying concentrations of benzbromarone

Data were fit to a two-site model (see eq. 1). Parameter estimates are reported as the estimate (mean ± S.E. of the estimate) resulting from nonlinear regression of the data. K_B, the binding constant for the effector; α, the change in K_m resulting from effector binding; and β, the change in V_m resulting from effector binding. An α value <1 indicates a decrease in K_m. A β value >1 indicates an increase in V_m, whereas a β value <1 indicates a decrease in V_m.

Enzyme	V_m	K_m	K_B	α	β	R^2
	pmol/min/pmol P450	*μM*	*nM*			
CYP2C9.1	3.98 (0.13)	16.4 (1.98)	39.9 (14.2)	5.02 (1.94)	0.50 (0.13)	0.977
CYP2C9.3	1.43 (0.09)	147 (20.6)	627 (516)	0.14 (0.08)	1.14 (0.11)	0.991

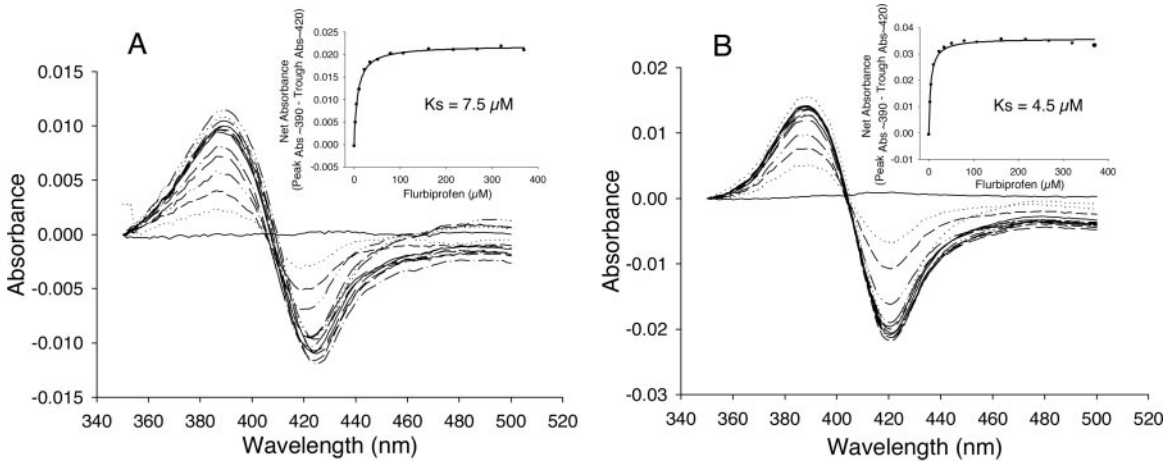

Fig. 3. Binding spectra of flurbiprofen to CYP2C9.1 alone (A) and in the presence of 300 nM benzbromarone (B). Inset graph is the fit of the spectral difference data used to determine the K_s.

heme iron in CYP2C9.3 (I359L) as in CYP2C9.1, despite reduced substrate turnover by the variant enzyme. The plots of $1/T_{1P}$ versus 1/temperature for the T_1 relaxation studies for CYP2C9.1 and CYP2C9.3 exhibited a positive linear slope for all of the protons, indicating temperature dependence and thus fast exchange (data not shown).

Docking of flurbiprofen and benzbromarone was conducted using the 1R9O crystal structure of CYP2C9 (Wester et al., 2004). Depictions of lowest energy conformations of benzbromarone docked within the active site, while maintaining flurbiprofen oriented near the heme iron, are presented in Fig. 5, A and B. Although the space directly above the heme is occupied by flurbiprofen and further constricted by residues Leu362 and Leu366, suitable space for docking of benzbromarone was found above flurbiprofen (Fig. 5, A and B). Maintaining flurbiprofen closest to the heme, benzbromarone populated two overlapping positions that together covered most of the major substrate recognition sites (SRS regions), including the B–C loop, the F, G, and I helices, and the C-terminal loop containing Phe476. Both positions of benz-

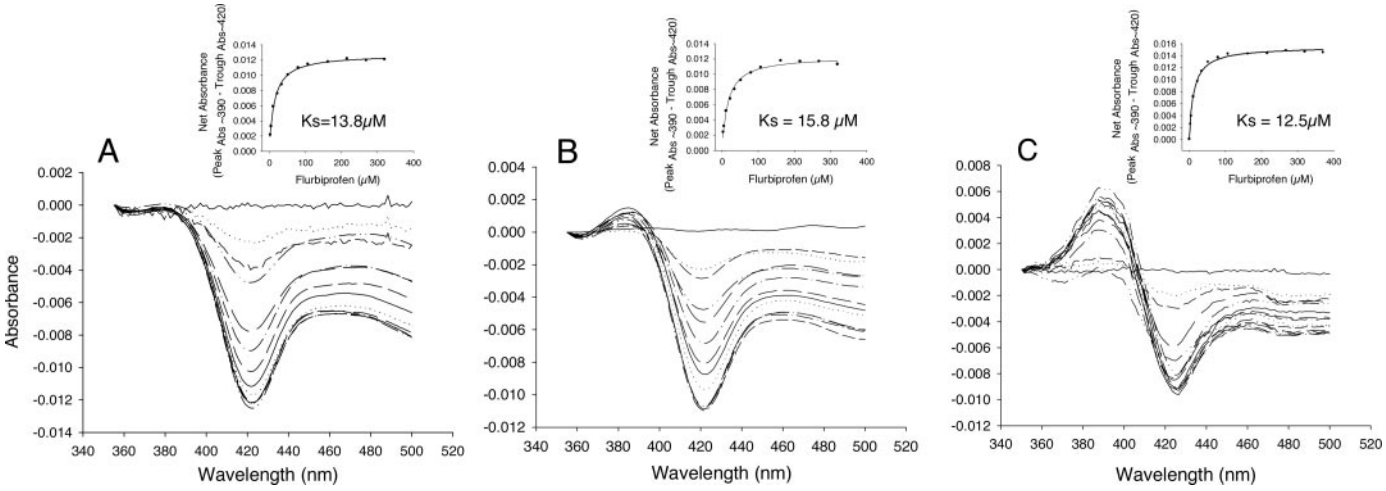

Fig. 4. Binding spectra of flurbiprofen to CYP2C9.3 alone (A) in the presence of 100 nM benzbromarone (B) and in the presence of 300 nM benzbromarone (C). Inset graph is the fit of the spectral difference data used to determine the K_s.

TABLE 2

T_1 relaxation rate-estimated distances of flurbiprofen protons from the heme iron of CYP2C9.1 in the absence and presence of 300 nM benzbromarone

Errors for measurements are shown within parentheses. Errors in the T_1 values were those reported by the fitting routine. Errors in the reported distances (r) were determined by propagation of error from the T_1 calculation. Flurbiprofen concentration was 145 μM; benzbromarone concentration was 300 nM when studied together. See Fig. 1 for the numbering scheme of the flurbiprofen protons. T_1 calculations for the HC-CO_2H proton could not be accurately determined because of interference from the residual glycerol resonances. T_1 values are in seconds. [P450 2C9] = 0.014 μM; $\alpha_M = [P450]/(K_s + [substrate])$, K_S (flurbiprofen) = 7.8 μM, α_M (flurbiprofen) = 9.16×10^{-5}. Distance values are in angstroms (Å), $r = C[T_{1P} \times \alpha_M \times f(\tau_c)]^{-1/6}$, $C = 539$ (Mildvan and Gupta, 1978), $1/T_{1P} = 1/T_{1,\ 2C9} - 1/T_{1,\ 2C9\ +\ CO}$ (Mildvan and Gupta, 1978), $f(\tau_c) = 2 \times 10^{-10}\ s^{-1}$.

Proton	CYP2C9.1			CYP2C9.1 with Benzbromarone		
	2C9	2C9 + CO	r	2C9	2C9 + CO	r
2′,6′	2.46 (0.03)	2.83 (0.03)	4.52 (0.06)	2.41 (0.03)	2.83 (0.04)	4.41 (0.07)
3′,5′	2.49 (0.03)	2.85 (0.03)	4.53 (0.06)	2.49 (0.03)	2.85 (0.03)	4.53 (0.06)
5	2.22 (0.05)	2.43 (0.05)	4.77 (0.11)	2.12 (0.06)	2.64 (0.06)	4.12 (0.12)
4′	3.86 (0.16)	4.67 (0.19)	4.65 (0.19)	3.32 (0.10)	4.43 (0.21)	4.27 (0.21)
6	1.95 (0.03)	2.20 (0.04)	4.46 (0.07)	1.92 (0.05)	2.16 (0.04)	4.46 (0.13)
2	2.67 (0.06)	3.15 (0.08)	4.45 (0.11)	2.54 (0.08)	3.13 (0.10)	4.28 (0.14)
CH_3	0.71 (0.01)	0.73 (0.01)	4.76 (0.04)	0.69 (0.01)	0.72 (0.01)	4.44 (0.05)

TABLE 3

T_1 relaxation rate-estimated distances of flurbiprofen protons from the heme iron of CYP2C9.3 in the absence and presence of 300 nM benzbromarone

Errors for measurements are shown in parentheses. Errors in the T_1 values were those reported by the fitting routine. Errors in the reported distances (r) were determined by propagation of error from the T_1 calculation. Flurbiprofen concentration was 300 μM; benzbromarone concentration was 300 nM when studied together. See Fig. 1 for the numbering scheme of the flurbiprofen protons. T_1 calculations for the HC-CO_2H proton could not be accurately determined because of interference from the residual glycerol resonances. T_1 values are in seconds. [P450 2C9] = 0.014 μM; $\alpha_M = [P450]/(K_s + [substrate])$, K_S (flurbiprofen) = 13.8 μM, α_M (Flurbiprofen) = 9.16×10^{-5}. Distance values are in angstroms (Å), $r = C[T_{1P} \times \alpha_M \times f(\tau_c)]^{-1/6}$, $C = 539$ (Mildvan and Gupta, 1978), $1/T_{1P} = 1/T_{1,\ 2C9} - 1/T_{1,\ 2C9\ +\ CO}$ (Mildvan and Gupta, 1978), $f(\tau_c) = 2 \times 10^{-10}\ s^{-1}$.

Proton	CYP2C9.3			CYP2C9.3 with Benzbromarone		
	2C9	2C9 + CO	r	2C9	2C9 + CO	r
2′,6′	2.40 (0.02)	2.78 (0.03)	4.50 (0.04)	2.41 (0.02)	2.79 (0.02)	4.50 (0.39)
3′,5′	2.43 (0.02)	2.84 (0.03)	4.46 (0.04)	2.44 (0.03)	2.85 (0.03)	4.47 (0.05)
5	2.13 (0.04)	2.44 (0.05)	4.46 (0.10)	2.16 (0.03)	2.46 (0.04)	4.49 (0.08)
4′	3.44 (0.07)	4.18 (0.14)	4.57 (0.15)	3.82 (0.12)	4.88 (0.18)	4.50 (0.16)
6	1.96 (0.03)	2.14 (0.04)	4.74 (0.08)	1.95 (0.03)	2.16 (0.03)	4.62 (0.06)
2	2.66 (0.04)	3.06 (0.07)	4.61 (0.11)	2.64 (0.05)	3.11 (0.06)	4.50 (0.09)
CH_3	0.68 (0.01)	0.70 (0.01)	4.89 (0.06)	0.69 (0.01)	0.71 (0.01)	4.79 (0.06)

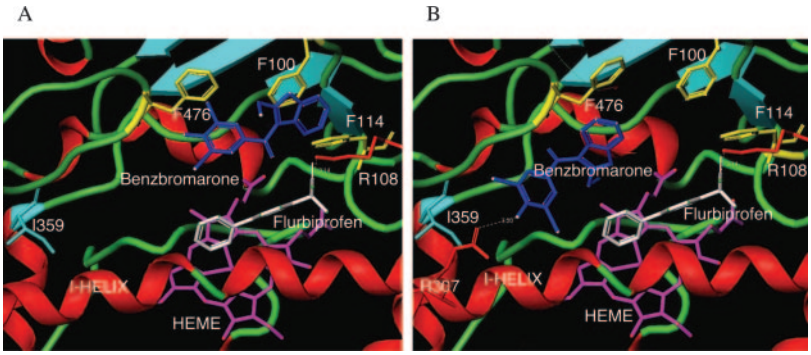

Fig. 5. A and B, potential docking locations and energy minimized flurbiprofen and benzbromarone within the active site of CYP2C9 based on the 1R90 crystal structure of CYP2C9. Flurbiprofen is colored white, and benzbromarone is colored blue.

bromarone also overlap the docked position of dapsone (Wester et al., 2004).

Discussion

Prediction of drug interactions resulting from P450 inhibition may be confounded by many factors. The ability of P450 enzymes, such as CYP2C9, to accommodate multiple substrate molecules within their active sites can affect interactions between substrates (Korzekwa et al., 1998; Hutzler et al., 2001; Tracy et al., 2002; Wienkers, 2002), resulting in substrate-dependent inhibition. CYP2C9 also exhibits genetic polymorphisms that contribute to interindividual variability in metabolism rates (Haining et al., 1996; Takanashi et al., 2000; Dickmann et al., 2001; Tracy et al., 2002), yet little is known regarding whether CYP2C9 polymorphisms might also affect the degree of inhibition-based drug-drug interactions. To this end, the inhibition of flurbiprofen by benzbromarone, the most potent inhibitor of CYP2C9 reported so far, was tested in CYP2C9.1 and CYP2C9.3 to examine whether variant-dependent inhibition exists for these enzymes. In contrast to its inhibitory effect in CYP2C9.1, in the CYP2C9.3 enzyme, benzbromarone was a potent activator of flurbiprofen metabolism. This unexpected finding suggests that the extent and type of drug interaction observed may be dependent on the genotype of a person, further complicating the potential for predicting drug-drug interactions.

As predicted, the turnover of flurbiprofen by CYP2C9.3 is greatly reduced compared with wild-type enzyme. Thus, it was surprising that benzbromarone, a potent inhibitor of this same process in wild-type enzyme, activated flurbiprofen hydroxylation in the CYP2C9.3 variant; a complete reversal of effect. Other activators of CYP2C9-mediated flurbiprofen metabolism, such as dapsone and selected analogs, have been identified, but these compounds exhibit activation kinetics, regardless of the CYP2C9 variant studied (Hummel et al., 2004a). Marks et al. (2004) have reported a similar change from inhibition to activation for ibuprofen inhibition of Vivid Red metabolism by CYP2C9.1 and CYP2C9.3, respectively. However, this occurred at micromolar ibuprofen concentrations as opposed to the nanomolar concentrations observed with benzbromarone. Studying amiodarone, a compound structurally related to benzbromarone, Egnell et al. (2003) observed that amiodarone, which is typically a weak inhibitor of CYP2C9 metabolism, activated 7-methoxyfluorocoumarin metabolism at nanomolar concentrations. However, this phenomenon was only studied with the wild-type CYP2C9 enzyme.

To examine the reasons underlying the benzbromarone-induced switching to activation kinetics in the variant CYP2C9.3 enzyme, several additional studies were conducted. T_1 relaxation NMR studies can be used to estimate substrate proton to heme iron distances of cytochrome P450 enzymes (Regal and Nelson, 2000; Hummel et al., 2004b). Thus, we studied the distances of flurbiprofen protons from the heme iron in both the CYP2C9.1 and CYP2C9.3 enzymes in the absence and presence of benzbromarone. In the presence of benzbromarone, the time-averaged distances of flurbiprofen protons from the heme of CYP2C9.1 were relatively unaffected by the presence of benzbromarone. This is presumed to be due to the mutual exclusivity of flurbiprofen or to benzbromarone being near enough to the heme iron for measurement of distances. Likewise, benzbromarone had no substantial effect on distances of the flurbiprofen protons relative to the heme iron in CYP2C9.3. This finding differs from that observed in the activation of flurbiprofen metabolism by dapsone with the CYP2C9.1 enzyme (Hummel et al., 2004b). Thus, changes in flurbiprofen proton to heme iron distances do not seem to account for the activation of flurbiprofen metabolism by benzbromarone in CYP2C9.3. Unfortunately, we were unable to measure the T_1 relaxation of the benzbromarone protons because of the large abundance of flurbiprofen (300 μM flurbiprofen versus 300 nM benzbromarone) in the sample, which prevented resolution of the resonances for benzbromarone protons. This prevented us from definitively determining whether benzbromarone was simultaneously binding within the active site along with flurbiprofen. It is interesting to note that the distances of flurbiprofen alone in CYP2C9.3 are similar to the distances of flurbiprofen observed in CYP2C9.1. This result suggests that, even though the flurbiprofen protons are at a similar distance from the heme iron when bound to CYP2C9.3 compared with CYP2C9.1, it either assumes a less productive orientation in the active site or that the CYP2C9.3 variant results in reduced substrate turnover through some mechanism other than change in substrate orientation.

To assess other possible reasons for the observed switching of benzbromarone effect, the binding affinity (K_s) of flurbiprofen for each of the two enzymes (CYP2C9.1 and CYP2C9.3) was determined in the absence and presence of benzbromarone. Benzbromarone coincubation caused a modest change in flurbiprofen-binding affinity in CYP2C9.1 but no change in CYP2C9.3, despite the observed changes in turnover. This phenomenon of activation without a corresponding increase in binding affinity is analogous to that observed with *N*-hydroxydapsone activation of flurbiprofen

hydroxylation in CYP2C9.1 (Hutzler et al., 2003) and contrasts with the increase in flurbiprofen-binding affinity with dapsone. These results reinforce previous observations that the activation of cytochrome P450-mediated metabolism may occur through multiple mechanisms and that the mechanisms involved can be dependent on effector or enzyme.

It is interesting that the measurement of difference spectra in the case of CYP2C9.3 gave somewhat unusual results (Fig. 4, A–C). It is possible that the K_s of flurbiprofen does change in the presence of benzbromarone but that the abnormal difference spectra obscured this change. Upon titration of flurbiprofen, 2C9.3 failed to give a measurable increase in the 390-nm peak of the difference spectra associated with conversion of the heme iron from low spin to high spin (Fig. 4A). When benzbromarone was added during the titrations (Fig. 4, B and C), the 390-nm peak appeared, whereas the negative low-spin peak at 420 nm reached its minimum at the same concentration of flurbiprofen in every experiment. This suggests that the K_s determination was not affected by the anomalous nature of the 390-nm peak of the difference spectra. All of the difference spectra of P450s taken after the addition of ligand result from perturbation of the solvent network near the distal face of the heme or coordination to the iron. Unfortunately, the precise reason for the variable difference spectra in the 390-nm region is currently unknown and perhaps is better explored using other methods (e.g., EPR). Whether this phenomenon is associated with altered enzyme activity (e.g., that of CYP2C9.3) is unclear, because the CYP2C9 substrate diclofenac produces only modest changes in the high-spin peak relative to the decrease in the low-spin peak (M. A. Hummel, C. W. Locuson, P. M. Gannett, D. A. Rock, C. Mosher, A. E. Rettie, and T. S. Tracy, unpublished observations) yet exhibits a high k_{cat} value similar to that of flurbiprofen (Dickmann et al., 2001).

To gain additional insight into the binding orientation for benzbromarone, docking studies were performed with the wild-type enzyme. Although the docking carried out does not allow the movement of the enzyme in any manner, it demonstrates that there is sufficient space for heteroactivator binding within the same active site as the substrate. In addition, the Ile359 residue, which is conservatively changed to leucine in CYP2C9.3, has no way of directly contacting either substrate or effector, despite switching of benzbromarone effect to activation in the CYP2C9.3 enzyme. The leucine at position 359 may alter adjacent residue side chain packing so that the enzyme gains the volume or flexibility to accommodate benzbromarone in a different orientation than in wild-type enzyme, causing an enhancement of flurbiprofen metabolism. Examining a series of benzbromarone analogs to probe the CYP2C9-active site, Locuson et al. (2003, 2004) proposed that benzbromarone binds in CYP2C9 by interacting edge-to-face with Phe114 and ion pairing with Arg108. Arg108 was also found to be important for obtaining a type I-binding spectrum for both flurbiprofen and benzbromarone (Dickmann et al., 2004). This Arg108 residue binding of benzbromarone probably results in benzbromarone inhibition of flurbiprofen metabolism, because both molecules would compete for this Arg residue in CYP2C9.1. In the case of CYP2C9.3, perhaps the phenol of the benzbromarone or the carboxylic acid of flurbiprofen is able to bind more readily to another positively charged residue in CYP2C9.3 (Fig. 5B), reducing the competition for this binding orientation/site and enabling activation to occur.

Although this change in type of interaction is substrate-, effector-, and variant-dependent, it is an important finding, especially for low therapeutic window drugs, because roughly 10% of the white population carries at least one allele expressing CYP2C9.3 (Lee et al., 2002). For example, a patient homozygous for CYP2C9.3 may empirically have their dose lowered because of the coadministration of a CYP2C9 inhibitor. However, if the CYP2C9.1 inhibitor activates CYP2C9.3, the amount of parent drug in the body would be reduced, thereby decreasing efficacy in contrast to what would be expected with inhibition. In addition, intentional activating drug-drug interactions could conceivably prove useful in altering drug plasma levels to treat overdoses or increase active metabolite production depending on one's genetics.

In summary, CYP2C9.1-mediated flurbiprofen metabolism was inhibited by the presence of benzbromarone, whereas CYP2C9.3-mediated flurbiprofen metabolism was activated by coincubation with this same effector. This seemingly modest amino acid substitution (I359L) may alter active site conformation and/or substrate/effector binding in such a way that it results in the switching of effect from inhibition to activation. Results, such as these demonstrating alterations in drug interaction effects in variant P450 enzymes, will undoubtedly further complicate prediction of drug interactions in the early stages of drug development.

References

Barnes HJ, Arlotto MP, and Waterman MR (1991) Expression and enzymatic activity of recombinant cytochrome P450 17 alpha-hydroxylase in *Escherichia coli*. *Proc Natl Acad Sci USA* **88:**5597–5601.

Cheesman MJ, Baer BR, Zheng YM, Gillam EM, and Rettie AE (2003) Rabbit CYP4B1 engineered for high-level expression in *Escherichia coli*: ligand stabilization and processing of the N-terminus and heme prosthetic group. *Arch Biochem Biophys* **416:**17–24.

Dickmann LJ, Locuson CW, Jones JP, and Rettie AE (2004) Differential roles of Arg97, Asp293, and Arg108 in enzyme stability and substrate specificity of CYP2C9. *Mol Pharmacol* **65:**842–850.

Dickmann LJ, Rettie AE, Kneller MB, Kim RB, Wood AJ, Stein CM, Wilkinson GR, and Schwarz UI (2001) Identification and functional characterization of a new CYP2C9 variant (CYP2C9*5) expressed among African Americans. *Mol Pharmacol* **60:**382–387.

Egnell AC, Eriksson C, Albertson N, Houston B, and Boyer S (2003) Generation and evaluation of a CYP2C9 heteroactivation pharmacophore. *J Pharmacol Exp Ther* **307:**878–887.

Galetin A, Clarke SE, and Houston JB (2002) Quinidine and haloperidol as modifiers of CYP3A4 activity: multisite kinetic model approach. *Drug Metab Dispos* **30:**1512–1522.

Haining RL, Hunter AP, Veronese ME, Trager WF, and Rettie AE (1996) Allelic variants of human cytochrome P450 2C9: baculovirus-mediated expression, purification, structural characterization, substrate stereoselectivity and prochiral selectivity of the wild-type and I359L mutant forms. *Arch Biochem Biophys* **333:**447–458.

Haining RL, Jones JP, Henne KR, Fisher MB, Koop DR, Trager WF, and Rettie AE (1999) Enzymatic determinants of the substrate specificity of CYP2C9: role of B′-C loop residues in providing the Pi-stacking anchor site for warfarin binding. *Biochemistry* **38:**3285–3292.

Higashi MK, Veenstra DL, Kondo LM, Wittkowsky AK, Srinouanprachanh SL, Farin FM, and Rettie AE (2002) Association between CYP2C9 genetic variants and anticoagulation-related outcomes during warfarin therapy. *J Am Med Assoc* **287:**1690–1698.

Hummel MA, Dickmann LJ, Rettie AE, Haining RL, and Tracy TS (2004a) Differential activation of CYP2C9 variants by dapsone. *Biochem Pharmacol* **67:**1831–1841.

Hummel MA, Gannett PM, Aguilar JS, and Tracy TS (2004b) Effector-mediated alteration of substrate orientation in cytochrome P450 2C9. *Biochemistry* **43:**7207–7214.

Hutzler JM, Hauer MJ, and Tracy TS (2001) Dapsone activation of CYP2C9-mediated metabolism: evidence for activation of multiple substrates and a two-site model. *Drug Metab Dispos* **29:**1029–1034.

Hutzler JM, Wienkers LC, Wahlstrom JL, Carlson TJ, and Tracy TS (2003) Activation of cytochrome P450 2C9-mediated metabolism: mechanistic evidence in support of kinetic observations. *Arch Biochem Biophys* **410:**16–24.

Korzekwa KR, Krishnamachary N, Shou M, Ogai A, Parise RA, Rettie AE, Gonzalez FJ, and Tracy TS (1998) Evaluation of atypical cytochrome P450 kinetics with

two-substrate models: evidence that multiple substrates can simultaneously bind to cytochrome P450 active sites. *Biochemistry* **37:**4137–4147.
Lee CR, Goldstein JA, and Pieper JA (2002) Cytochrome P450 2C9 Polymorphisms: a Comprehensive Review of the in-Vitro and Human Data. *Pharmacogenetics* **12:**251–263.
Locuson CW, Rock DA, and Jones JP (2004) Quantitative binding models for CYP2C9 based on benzbromarone analogues. *Biochemistry* **43:**6948–6958.
Locuson CW, Wahlstrom JL, Rock DA, Rock DA, and Jones JP (2003) A new class of CYP2C9 inhibitors: probing 2C9 specificity with high-affinity benzbromarone derivatives. *Drug Metab Dispos* **31:**967–971.
Marks BD, Thompson DV, Goossens TA, and Trubetskoy OV (2004) High-throughput screening assays for the assessment of CYP2C9*1, CYP2C9*2, and CYP2C9*3 metabolism using fluorogenic vivid substrates. *J Biomol Screen* **9:**439–449.
Mildvan AS and Gupta RK (1978) Nuclear relaxation measurements of the geometry of enzyme-bound substrates and analogs. *Methods Enzymol* **49:**322–359.
Modi S, Paine MJ, Sutcliffe MJ, Lian LY, Primrose WU, Wolf CR, and Roberts GC (1996) A model for human cytochrome P450 2D6 based on homology modeling and NMR studies of substrate binding. *Biochemistry* **35:**4540–4550.
Nakamura H, Nakasa H, Ishii I, Ariyoshi N, Igarashi T, Ohmori S, and Kitada M (2002) Effects of endogenous steroids on CYP3A4-mediated drug metabolism by human liver microsomes. *Drug Metab Dispos* **30:**534–540.
Poli-Scaife S, Attias R, Dansette PM, and Mansuy D (1997) The substrate binding site of human liver cytochrome P450 2C9: an NMR study. *Biochemistry* **36:**12672–12682.
Regal KA and Nelson SD (2000) Orientation of caffeine within the active site of human cytochrome P450 1A2 based on NMR longitudinal (T1) relaxation measurements. *Arch Biochem Biophys* **384:**47–58.
Shafirovich V, Mock S, Kolbanovskiy A, and Geacintov NE (2002) Photochemically catalyzed generation of site-specific 8-nitroguanine adducts in DNA by the reaction of long-lived neutral guanine radicals with nitrogen dioxide. *Chem Res Toxicol* **15:**591–597.
Shou M, Dai R, Cui D, Korzekwa KR, Baillie TA, and Rushmore TH (2001) A kinetic model for the metabolic interaction of two substrates at the active site of cytochrome P450 3A4. *J Biol Chem* **276:**2256–2262.
Shou M, Grogan J, Mancewicz JA, Krausz KW, Gonzalez FJ, Gelboin HV, and Korzekwa KR (1994) Activation of CYP3A4: evidence for the simultaneous binding of two substrates in a cytochrome P450 active site. *Biochemistry* **33:**6450–6455.
Shou M, Mei Q, Ettore MW Jr, Dai R, Baillie TA, and Rushmore TH (1999) Sigmoidal kinetic model for two co-operative substrate-binding sites in a cytochrome P450 3A4 active site: an example of the metabolism of diazepam and its derivatives. *Biochem J* **340:**845–853.
Steward DJ, Haining RL, Henne KR, Davis G, Rushmore TH, Trager WF, and Rettie AE (1997) Genetic association between sensitivity to warfarin and expression of CYP2C9*3. *Pharmacogenetics* **7:**361–367.
Takanashi K, Tainaka H, Kobayashi K, Yasumori T, Hosakawa M, and Chiba K (2000) CYP2C9 Ile359 and Leu359 variants: enzyme kinetic study with seven substrates. *Pharmacogenetics* **10:**95–104.
Tracy TS, Hutzler JM, Haining RL, Rettie AE, Hummel MA, and Dickmann LJ (2002) Polymorphic variants (CYP2C9*3 and CYP2C9*5) and the F114L active site mutation of CYP2C9: effect on atypical kinetic metabolism profiles. *Drug Metab Dispos* **30:**385–390.
Tracy TS, Marra C, Wrighton SA, Gonzalez FJ, and Korzekwa KR (1996) Studies of flurbiprofen 4′-hydroxylation—additional evidence suggesting the sole involvement of cytochrome P450 2C9. *Biochem Pharmacol* **52:**1305–1309.
Tracy TS, Rosenbluth BW, Wrighton SA, Gonzalez FJ, and Korzekwa KR (1995) Role of cytochrome P450 2C9 and an allelic variant in the 4′-hydroxylation of (*R*)- and (*S*)-flurbiprofen. *Biochem Pharmacol* **49:**1269–1275.
Wester MR, Yano JK, Schoch GA, Yang C, Griffin KJ, Stout CD, and Johnson EF (2004) The structure of human cytochrome P450 2C9 complexed with flurbiprofen at 2.0-Å resolution. *J Biol Chem* **279:**35630–35637.
Wienkers LC (2002) Factors confounding the successful extrapolation of in vitro CYP3A inhibition information to the in vivo condition. *Eur J Pharm Sci* **15:**239–242.
Williams PA, Cosme J, Ward A, Angove HC, Matak VD, and Jhoti H (2003) Crystal structure of human cytochrome P450 2C9 with bound warfarin. *Nature (Lond)* **424:**464–468.
Yamazaki H, Inoue K, Chiba K, Ozawa N, Kawai T, Suzuki Y, Goldstein JA, Guengerich FP, and Shimada T (1998) Comparative studies on the catalytic roles of cytochrome P450 2C9 and its Cys- and Leu-variants in the oxidation of warfarin, flurbiprofen and diclofenac by human liver microsomes. *Biochem Pharmacol* **56:**243–251.

Address correspondence to: Dr. Timothy S. Tracy, Department of Experimental and Clinical Pharmacology, College of Pharmacy, University of Minnesota, 308 Harvard St., S.E., Minneapolis, MN 55455. E-mail: tracy017@umn.edu